Inorganic Chemistry

COMMUNICATION

pubs.acs.org/IC

NCN-Chelated Organoantimony(III) and Organobismuth(III) Phosphates: Synthesis and Solid-State and Solution Structures

Tomáš Svoboda,[†] Libor Dostál,[*,†] Roman Jambor,[†] Aleš Růžička,[†] Robert Jirásko,[‡] and Antonín Lyčka[⊥]

[†]Department of General and Inorganic Chemistry, [‡]Department of Analytical Chemistry, Faculty of Chemical Technology, University of Pardubice, Studentská 573, Pardubice, CZ-53210, Czech Republic

[⊥]Research Institute for Organic Syntheses, Rybitví 296, CZ-53354 Pardubice, Czech Republic

Supporting Information

ABSTRACT: .Organoantimony(III) and organobismuth(III) phosphates $(LM)_3(PO_4)_2$ [M = Sb (**3**) and Bi (**4**)], containing the NCN-chelating ligand L [L = 2,6-$(CH_2NMe_2)_2C_6H_3$], were prepared by the simple treatment of parent oxides **1** and **2** with H_3PO_4. Both compounds were characterized by elemental analysis, electrospray ionization mass spectrometry, and IR and NMR spectroscopy and in the case of **3** by X-ray diffraction techniques. Compound **3** has an interesting behavior in solution, i.e., the formation of two possible conformational isomers, which was studied by ^1H, ^{13}C, and ^{31}P NMR spectroscopy.

The antimony orthophosphate $SbPO_4$ may be prepared by the reaction[1] of antimony oxide (valentine polymorph) with H_3PO_4 and consists of sheets of PO_4 tetrahedra and SbO_4 polyhedra, which are connected to an infinite network.[2] This phosphate was shown to be able to intercalate various organic molecules without the destruction of its layered framework[3] and was studied as a potential anode in lithium-ion batteries.[4] Three different modifications of crystalline $BiPO_4$ are known, of which the monazite type is thermodynamically most favored.[5] This compound has been studied with regard to its potential application in catalysis[6] and separation of radioactive actinides[7] and as a host for the incorporation of luminescence rare-earth ions.[8]

Recently, we have demonstrated that using NCN-chelated organoantimony and organobismuth oxides $[LMO]_2$ [M = Sb (**1**)[9] and Bi (**2**)],[10] where L is the designation for the [2,6-$(CH_2NMe_2)_2C_6H_3$] ligand (Scheme 1), as well-defined and soluble precursors provides an elegant synthetic pathway for the preparation of a variety of phosphorus-containing compounds such as phosphonates, phosphites, or phosphinates.[11] The majority of these compounds were prepared by the simple treatment of the starting oxides with corresponding acids under elimination of water. We wonder if the corresponding reaction with H_3PO_4 acid follows the same reaction path and gives well-defined molecular antimony and bismuth phosphates. Thus, we report here on the reactions of oxides **1** and **2** with H_3PO_4, which lead smoothly to the corresponding phosphates $(LM)_3(PO_4)_2$ [M = Sb (**3**) and Bi (**4**)], and describe their structure both in the solid state and in solution.

The treatment of organoantimony and organobismuth oxides **1** and **2** with H_3PO_4 in toluene according to Scheme 1 afforded target compounds **3** and **4** as air-stable white solids in good yield.

Scheme 1. Preparation of Compounds 3 and 4

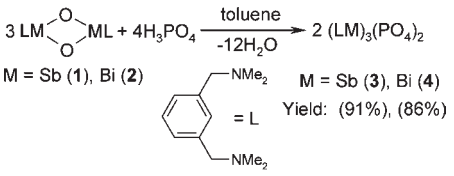

Noteworthy is the fact that full deprotonation of the H_3PO_4 acid does not require the addition of any base pointing to high basic properties of both oxides under the reaction conditions. Compounds **3** and **4** are soluble in aromatic (moderately), chlorinated solvents as well as in tetrahydrofuran. The identity of both compounds was established by elemental analysis and electrospray ionization mass spectrometry. The formation of protonated molecules of **3** and **4** ($[M + H]^+$), providing information about the molecular weight (MW), is the most important ionization mechanism in the full-scan positive-ion mass spectra of the studied compounds **3** and **4**. Their tandem mass spectra show the fragment ions $[(LM)_2(PO_4)]^+$ formed by the neutral loss of $(LM)(HPO_4)$ (see the Supporting Information). The presence of phosphate moieties in the structures of **3** and **4** was corroborated by the observation of characteristic vibrational bands in the PO_4 vibrational domain in their respective IR spectra.

The molecular structure of **3** was unambiguously established by the X-ray diffraction studies;[12] unfortunately, all attempts to grow suitable single crystals of **4** failed up until this moment. Compound **3** crystallizes as a solvate either as $3\cdot 2H_2O\cdot 3CH_2Cl_2$ (**3a**; Figures 1 and 2) or as $3\cdot H_2O\cdot 1.5C_7H_8$ (**3b**; see the Supporting Information). Nevertheless, the cores containing the antimony atoms, ligands L, and phosphate moieties in **3a** and **3b** are nearly identical (regarding the structural parameters) in both cases; thus, only **3a** is described here; for details about **3b**, see the Supporting Information.

Two phosphate moieties are bridged by three LSb fragments, which are symmetrically arranged around the central girdle (see Figure 1). The Sb−O bond distances fall within the narrow interval 2.044(3)−2.068(3) Å, and these values are close to the value for Sb−O covalent bonds [Σ_{cov}(Sb,O) = 2.02 Å]. There are two terminal P−O bonds within the phosphate moieties with the bond distance 1.494(4) Å, which is in accordance with the double

Received: May 2, 2011
Published: June 13, 2011

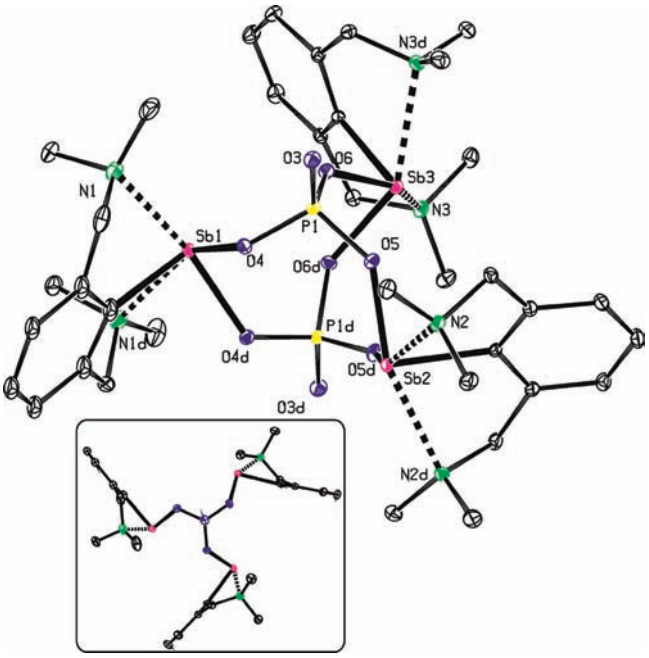

Figure 1. ORTEP plot of a molecule of **3a**, the top view along the P1−P1d axis, and the atom numbering scheme (symmetry code d: $x, y, 1 - z$). Solvent molecules (CH_2Cl_2 and H_2O) and hydrogen atoms were omitted for clarity. Selected bond lengths (Å) and angles (deg): Sb1−N1 2.647(4), Sb1−O4 2.068(3), Sb2−N2 2.637(4), Sb2−O5 2.044(3), Sb3−N3 2.593(4), Sb3−O6 2.068(3), P1−O3 1.494(3), P1−O4 1.555(3), P1−O5 1.544(3), P1−O6 1.550(3); N1−Sb1−N1d 115.26(12), N2−Sb2−N2d 117.75(11), N3−Sb3−N3d 116.28(11), O4−Sb1−O4d 82.62(12), O5−Sb2−O5d 84.99(13), O6−Sb3−O6d 83.57(12), Sb1−O4−P1 124.16(17), Sb2−O5−P1 139.77(19), Sb3−O6−P1 132.50(17), O4−P1−O3 111.22(18), O5−P1−O3 110.57(18), O6−P1−O3 112.13(18).

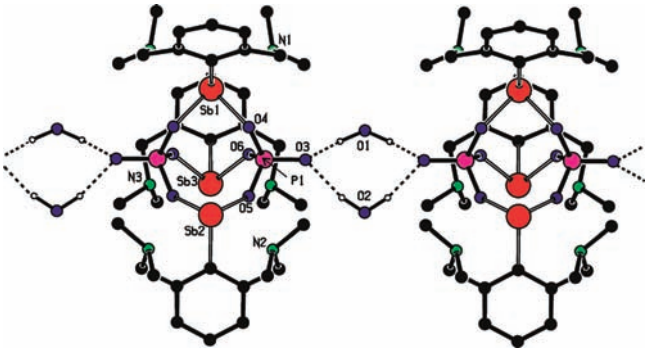

Figure 2. Infinite-chain structure of **3a** and the atom numbering scheme. Solvent molecules (CH_2Cl_2) and hydrogen atoms except those of water molecules were omitted for clarity. Selected bond lengths (Å) and angles (deg): O1−O3 2.906(5), O2−O3 2.866(5); O1−H(O1)−O3 153, O2−H(O2)−O3 160.

nature of this P═O bond. The remaining P−O(Sb) bond distances [1.544(3)−1.555(3) Å] are significantly longer. The phosphate moieties are mutually oriented into a nearly ideal eclipsed position along the P1−P1d axis. All of the nitrogen donor atoms of the ligands' pendant arms are coordinated to the central antimony atoms, with the Sb−N bond distances falling within the interval 2.593(4)−2.647(4) Å. Coordination of the ligands L may be described as pseudofacial, with the bonding N−Sb−N angles 115.26(12)−117.75(11)°. As a consequence of these Sb−N contacts, the coordination polyhedron around each antimony atom is a distorted square pyramid with the *ipso*-carbon atom in the apical position and nitrogen and oxygen atoms placed mutually in a cis fashion in the equatorial plane [corresponding O−Sb−O angles 82.62(12)−84.99(13)°].

The water molecules O1 and O2 are in contact through hydrogen bonds with the terminal P1−O3 bond in the crystal structure of **3a** (Figure 2). The bond distances describing these hydrogen bonds are O1−O3 2.906(5) Å and O2−O3 2.866(5) Å (the corresponding O−H−O bonding angles amount to 153 and 160°). The opposite apical P═O bond is involved in the same contacts with two water molecules, thus leading to the formation of infinite chains along the crystal structure of **3a**. Analogous hydrogen bonds between the P═O bonds and water can be seen also in the structure of **3b** (see the Supporting Information). In contrast to **3a**, **3b** forms only a monohydrate and only dimeric units connected via two water bridges are found in the crystal structure. This may be ascribed to the presence of only one water molecule available per each organometallic core; thus, further catenation of the dimeric units is hampered (see the Supporting Information).

The ^{1}H NMR data of **3** are identical regardless of whether single crystals or polycrystalline material is used for NMR analysis and revealed two sets for signals pointing to the presence of two compounds (conformational isomers vide infra) in solution.[13] Thus, the ^{1}H NMR spectrum of **3** in C_6D_6 contains a sharp AX pattern for CH_2N groups (major set of signals; see the Supporting Information) corresponding to the symmetric structure, where all three ligands L are equivalent. This finding corresponds to the solid-state structure (Figure1) and is designated as **3**-*sym* (Figure 3A). The second set of signals contains three AX patterns for three nonequivalent CH_2N groups (minor set of signals) in a mutual 1:1:1 integral ratio indicating the presence of a less symmetrical compound, where all three ligands are nonequivalent to each other.[14] The formation of such a structure can be easily rationalized by flipping of one of the ligands, leading to the nonequivalency of all three ligands and the formation of an asymmetric conformational isomer **3**-*asym* (Figure 3B).[14] These findings coincide with the ^{13}C NMR spectrum, where analogically four signals for CH_2N groups and aromatic carbon atoms, one for **3**-*sym* and three for **3**-*asym*, were obtained.

Another proof for the formation of both conformational isomers stems from ^{31}P NMR spectra, where two signals at −4.1 ppm (**3**-*sym*) and −7.9 ppm (**3**-*asym*) having a 1:0.2 intensity ratio were detected.[15] The situation is rather similar in the $CDCl_3$ solution, where two sets of signals attributable to the presence of **3**-*sym* and **3**-*asym* were detected in the ^{1}H NMR spectrum. More interestingly, the ratio between both isomers is strongly solvent-dependent because utilization of $CDCl_3$ resulted in a ratio between **3**-*sym* and **3**-*asym* of 1:0.91 (two signals in the ^{31}P NMR spectrum at −7.7 and −9.1 ppm). Again the ^{13}C NMR spectra in $CDCl_3$ revealed four signals for CH_2N groups and aromatic carbon atoms, which is in accordance with the presence of both **3**-*sym* and **3**-*asym*. Finally, we have proved that both isomers exist in equilibrium in solution by 2D ^{31}P−^{31}P *ex*change *s*pectroscop*y* (EXSY). Thus, there is a relatively slow exchange between forms **3**-*sym* and **3**-*asym*, as was clearly proved by the observation of an interaction between both phosphorus signals in the ^{31}P−^{31}P EXSY spectrum (Figure 4). An analogously

dx.doi.org/10.1021/ic2009144 |*Inorg. Chem.* 2011, 50, 6411–6413

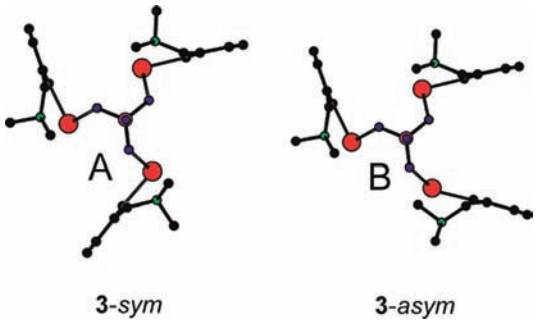

Figure 3. Schematic presentation of two conformational isomers of **3**, i. e., **3**-*sym* and **3**-*asym*.

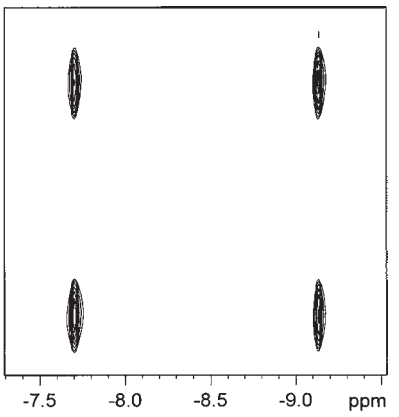

Figure 4. 2D $^{31}P-^{31}P$ EXSY spectrum of compound **3** in $CDCl_3$. Mixing time: 1s.

slow exchange between forms **3**-*sym* and **3**-*asym* in C_6D_6 was also proven using the same experimental technique.

In the case of the bismuth compound **4**, the ^1H NMR spectrum in C_6D_6 revealed only one AX pattern for CH_2N groups and two broadened signals for NMe_2 groups, and only one set of signals was obtained in the corresponding ^{13}C NMR spectrum. The ^{31}P NMR spectrum revealed only one signal at 2.42 ppm. These facts indicate, most probably because the molecular structure of **4** has not been determined, the presence of a symmetric structure **4**-*sym* in a benzene solution only, which is related to that of **3**-*sym*.

In conclusion, we have prepared unprecedented molecular organoantimony and organobismuth phosphates **3** and **4** by a straightforward reaction starting from oxides and H_3PO_4 and characterized them. Compound **3** displays an interesting conformational isomerism in solution, which is solvent-dependent. Studies dealing with similar mixed oxido compounds of group 15 elements are currently underway.

■ ASSOCIATED CONTENT

Supporting Information. All experimental details including synthesis descriptions, ^1H and ^{31}P NMR spectra, molecular structure of **3b**, all crystal data and structure refinement, atomic coordinates, anisotropic displacement parameters, and geometric data (CIF files). This material is available free of charge via the Internet at http://pubs.acs.org.

■ AUTHOR INFORMATION

Corresponding Author
*E-mail: libor.dostal@upce.cz.

■ ACKNOWLEDGMENT

The authors thank the GAČR (Grant P106/10/0443) and the Ministry of Education of the Czech Republic (Grants MSM0021627501 and MSM0021627502).

■ REFERENCES

(1) Sudarsan, V.; Muthe, K. P.; Vyas, J. C.; Kuhlshreshtha, S. K. *J. Alloys Compd.* **2002**, *336*, 119–123.
(2) Kinberge, B. *Acta Chem. Scand.* **1970**, *24*, 320.
(3) Saadaoui, H.; Bouchari, A.; Flandrois, S.; Aristides, J. *J. Mol. Cryst. Liq. Cryst.* **1994**, *224*, 173–178.
(4) Pena, J. S.; Pascual, J. C.; Caballero, A.; Morales, J.; Sánchez, L. *J. Solid State Chem.* **2004**, *177*, 2920–2927.
(5) (a) Mooney-Slater, R. C. L. *J. Chem. Phys.* **1984**, *16*, 1003. (b) Masse, R.; Durif, A. *C. R. Acad. Sci. Paris* **1985**, *300*, 849. (c) Romero, B.; Bruque, S.; Aranda, M. A. G.; Iglesias, J. E. *Inorg. Chem.* **1994**, *33*, 1869–1874.
(6) (a) Chang, T. S.; Li, G. J.; Shin, C. H.; Lee, Y. K.; Yun, S. S. *Catal. Lett.* **200**, *68*, 229–234. (b) Takita, Y.; Ninomiya, M.; Miyake, H.; Wakamatsu, H.; Yonshinaga, Y. *Phys. Chem. Chem. Phys.* **1999**, *1*, 4501–4504. (c) Delmon, B.; Ruwet, M.; Ceckiewicz, S. *Ind. Eng. Chem. Res.* **1987**, *26*, 1981–1983.
(7) Bond, A. H.; Nash, K. L.; Gelis, A. V.; Sullivan, J. C.; Jensen, M. P.; Rao, L. *Sep. Sci. Technol.* **2001**, *36*, 1241–1256.
(8) (a) Folkerts, H. F.; Zuidema, J.; Blasse, G. *Chem. Phys. Lett.* **1996**, *249*, 59–63. (b) Roming, M.; Feldmann, C. *J. Mater. Sci.* **2009**, *44*, 1412–1415.
(9) Dostál, L.; Jambor, R.; Růžička, A.; Erben, M.; Jirásko, R.; Černošková, Z.; Holeček, J. *Organometallics* **2009**, *28*, 2633–2636.
(10) Fridrichová, A.; Svoboda, T.; Jambor, R.; Paddlková, Z.; Růžička, A.; Erben, M.; Jirásko, R.; Dostál, L. *Organometallics* **2009**, *28*, 5522–5528.
(11) (a) Svoboda, T.; Jambor, R.; Růžička, A.; Paddlková, Z.; Erben, M.; Jirásko, R.; Dostál, L. *Eur. J. Inorg. Chem.* **2010**, 1663–1669. (b) Svoboda, T.; Jambor, R.; Růžička, A.; Paddlková, Z.; Erben, M.; Dostál, L. *Eur. J. Inorg. Chem.* **2010**, 5222–5230.
(12) **3a**: $3\cdot 2H_2O\cdot 3CH_2Cl_2$, M = 1419.88, orthorhombic, *Pbam*, colorless block, a = 20.4370(8) Å, b = 24.8581(19) Å, c = 11.1430(2) Å, V = 5660.9(13) Å^3, Z = 4, T = 150(1) K, 38 656 total reflections, 6734 independent (R_{int} = 0.031, R1 (obsd data) = 0.044, wR2 (all data) 0.097. CCDC 810313. **3b**: $3\cdot H_2O\cdot 1.5C_7H_8$, M = 1280.24, triclinic, $P\bar{1}$, colorless plate, a = 12.2120(8) Å, b = 13.6871(10) Å, c = 18.4900(9) Å, V = 2676.4(3) Å^3, Z = 2, T = 150(1) K, 52 950 total reflections, 12 239 independent (R_{int} = 0.034, R1 (obsd data) = 0.031, wR2 (all data) 0.064. CCDC 810314.
(13) Residual signals of the solvate molecule dichloromethane or toluene were obtained in the ^1H NMR spectra upon dissolving single crystals of **3a** and **3b**.
(14) Interestingly, analogous behavior has been very recently discovered and studied in the case of group 15 elements containing cryptands: (a) Cangelosi, V. M.; Zakharov, L. N.; Johnson, D. W. *Angew. Chem., Int. Ed.* **2010**, *49*, 1248–1251. (b) Cangelosi, V. M.; Carter, T. G.; Crossland, J. L.; Zakharov, L. N.; Johnson, D. W. *Inorg. Chem.* **2010**, *49*, 1248–1251.
(15) The integral ratio in ^1H and ^{31}P NMR spectra between both isomers is independent of the concentration of the NMR samples.